Resonant structures of overlapping doubly excited autoionization series in photoionization of Mg-like Al^{+} and Si^{2+} ions

T. K. Fang,[1] Baek Il Nam,[2] Young Soon Kim,[2] and T. N. Chang[1]
[1]*Department of Physics and Astronomy, University of Southern California, Los Angeles, California 90089-0484*
[2]*Department of Physics, Myong-Ji University, Yong-In 449-728, Seoul, Korea*
(Received 28 May 1996)

We present a quantitative study of the resonant structures of the overlapping $3p\nu d\ ^1F$ and $3p\nu g\ ^1F$ autoionization series in the photoionization from the bound excited ^1D states of Mg-like Al^{+} and Si^{2+} ions. The interference, both constructive and destructive, between the contributions from individual processes corresponding to transitions from specific initial to final-state configurations, are examined in detail. Our calculation shows that the photoionization from higher bound excited $3s\nu_i d\ ^1D$ state is dominated by the shakeup of the outer d electron following the $3s\rightarrow 3p$ core electron excitation. For Al^{+}, our calculation reveals the presence of a narrow $3p\nu g\ ^1F$ window resonance located on the higher-energy shoulder of its corresponding broad $3p\nu d\ ^1F$ resonance. Unlike the usual isolated window resonance, which is dominated by the transition from the initial state to the continuum component of the final-state wave function, the $3s\nu_i d\ ^1D\rightarrow 3p\nu g\ ^1F$ window resonance results primarily from the energy variation of the bound component, i.e., the weighted νd radial function, of the final-state wave function in the vicinity of the $3p\nu g\ ^1F$ resonance.
[S1050-2947(97)07301-0]

PACS number(s): 32.80.Fb, 32.80.Dz, 32.70.Jz, 31.25.Jf.

I. INTRODUCTION

For an *isolated* autoionization state with a resonant width Γ at resonant energy E_r, the resonant structure can be described by the Fano formula [1] in terms of an asymmetry parameter q. Qualitatively, the q parameter measures the interference between transitions from the initial state to the bound and continuum components of the final-state wave function. If the resonance is dominated by the contribution from the transition to the bound component of the final-state wave function, its corresponding q value is generally large and the resonant feature is approximately symmetric. If the contributions from transitions to both bound and continuum components of the final-state wave function are comparable, the resonant structure is asymmetric with an intermediate q value. If the spectrum is strongly dominated by the transition to the continuum component of the final-state wave function, a *window resonance* with zero cross section is expected either at or near the resonant energy E_r with $q\sim 0$.

The photoabsorption spectra from the $ns^2\ ^1S$ ground state of a divalent system (e.g., an alkaline-earth-metal atom) below the np threshold usually feature two asymmetric autoionization series, i.e., a broad $np\nu s\ ^1P$ and a narrow $np\nu d\ ^1P$ series, due to the simultaneous change of electronic orbitals of two outer electrons in a double-excitation process. Although the observed broad and narrow series may appear to overlap significantly [2], in principle, they are separated in energy since the outer νs and νd electrons differ substantially in their penetration to the smaller r region due to the difference in the repulsive centrifugal force. A recent study by Chang and Zhu [3,4] has indeed demonstrated that these two ^1P series can be separated unambiguously in the photoionization originated from the bound excited states. In contrast, for doubly excited autoionization series of higher orbital angular momentum, the quantum defects of the outer electrons become increasingly smaller due to the substantially higher centrifugal potential barrier. As a result, the broad and narrow doubly excited autoionization series may overlap significantly. It is the purpose of this study to examine in detail the interaction between a pair of overlapping $3p\nu d\ ^1F$ and $3p\nu g\ ^1F$ autoionization series in the photoionization of the Mg-like Al^{+} and Si^{2+} ions.

In Sec. II, we present the result of a B-spline-based configuration-interaction (BSCI) calculation [5,6] of the photoionization of Mg-like Al^{+} and Si^{2+} ions from their bound excited ^1D states to the strongly overlapping $3p\nu d\ ^1F$ and $3p\nu g\ ^1F$ autoionization series. For Al^{+}, we will identify a narrow $3p6g\ ^1F$ window resonance on the higher-energy shoulder of its corresponding broad $3s6d\ ^1D\rightarrow 3p6d\ ^1F$ resonance. For photoionization from highly excited $3s\nu_i d\ ^1D$ states, our calculation will show that the cross sections in the vicinity of the neighboring $3p\nu' g\ ^1F$ narrow resonances on the *higher*-energy side of the dominating $3s\nu_i d\ ^1D\rightarrow 3p\nu d\ ^1F$ resonance are consistently greater than the ones on the *lower*-energy side. In Sec. III, a detailed quantitative analysis of the contributions from individual transitions reveals that, unlike the usual isolated window resonance, the Al^{+} $3s\nu_i d\ ^1D\rightarrow 3p\nu g\ ^1F$ window

TABLE I. The dominating transitions and their corresponding transition amplitudes F_{fi}, including bound-to-bound (B-B) and bound-to-continuum (B-C) processes, that contribute significantly to the $^1D\rightarrow ^1F$ photoionization.

Transition	F_{fi}
$3s\nu_i d\rightarrow 3s\epsilon f$ (B-C)	$\langle \xi_{\nu_i d}\|r\|\xi_{\epsilon f}\rangle$
$3s\nu_i d\rightarrow 3p\nu d$ (B-B, shakeup)	$\langle \chi_{3s}\|r\|\chi_{3p}\rangle\langle \xi_{\nu_i d}\|\xi_{\nu d}\rangle$
$3p\nu_i p\rightarrow 3p\nu d$ (B-B)	$\langle \xi_{\nu_i p}\|r\|\xi_{\nu d}\rangle$
$3p\nu_i f\rightarrow 3p\nu g$ (B-B)	$\langle \xi_{\nu_i f}\|r\|\xi_{\nu g}\rangle$

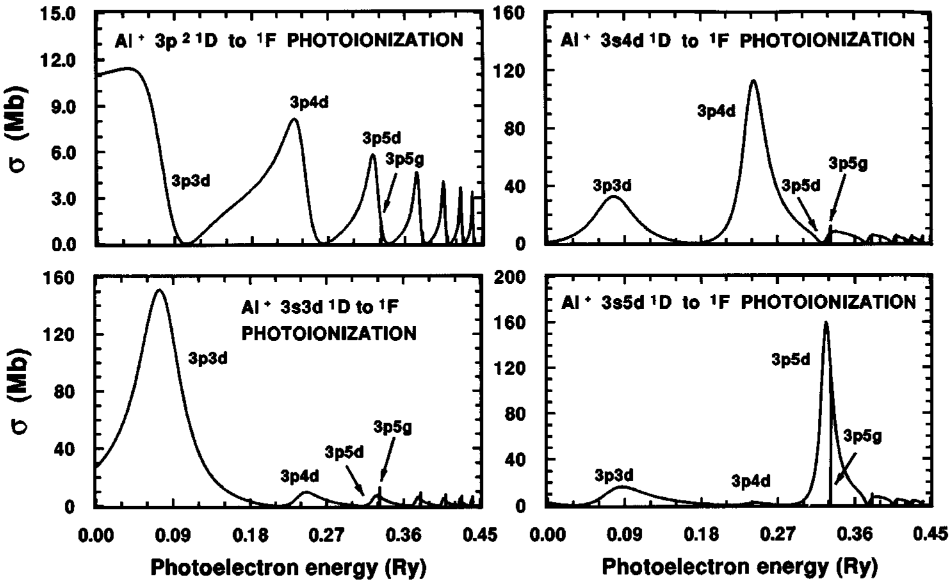

FIG. 1. Photoionization cross sections σ (in Mb) leading to the ^1F continuum from the bound excited ^1D states of Mg-like Al^+ ion.

resonance can be linked directly to the *shakeup* [4,7] of the outer d electron following the $3s \rightarrow 3p$ core electron excitation in the $3s\nu_i d\ ^1D \rightarrow 3p\nu d\ ^1F$ transition. The substantial difference in the magnitudes of the photoionization cross sections at energies below and above the dominating shakeup structure is due to the change from destructive to constructive interference between the individual contributions from transitions leading to the bound and continuum components of the final-state wave function.

II. RESULTS

Following the BSCI procedure outlined in [5,6], the ^1D initial state of the photoionization is dominated by the $3sd$, $3pp$, and $3pf$ configuration series and the ^1F final state is dominated by the $3sf$, $3pd$, and $3pg$ configuration series, or, schematically given by

$$\hbar\omega + \left\{ \begin{array}{l} 3sd\ ^1D \quad \text{(bound)} \\ 3pp\ ^1D \quad \text{(bound)} \\ 3pf\ ^1D \quad \text{(bound)} \end{array} \right\} \rightarrow \left\{ \begin{array}{c} 3sf\ ^1F \quad \text{(continuum)} \\ 3pd\ ^1F \quad \text{(bound)} \\ 3pg\ ^1F \quad \text{(bound)} \end{array} \right\}. \tag{1}$$

The total transition amplitude F^t_{fi} is the sum of transition amplitudes F_{fi} corresponding to all individual contributing processes. For the $^1D \rightarrow {}^1F$ photoionization of a Mg-like ion, the total amplitude F^t_{fi} is dominated by contributions from four processes listed in Table I. The one-electron orbital function $\chi_{\nu l}$ is normalized to unity. The weighted one-particle radial functions, i.e., $\xi_{\epsilon f}$ for the outgoing ϵf photoelectron and $\xi_{\nu l}$ for the bound electron representing the bound component of the $3p\nu l\ ^1F$ resonance, are defined by an expression similar to Eq. (50) of Ref. [6] or Eq. (10) of Ref. [5]. Similar to our recent photoionization calculations [4,8], a B-spline basis with a total number of 120 splines or larger is employed to represent the outgoing photoelectron. Approximately 5000 or more basis functions are included in our calculation. The length and velocity results typically agree to 3–4 % or better. Only the length results are presented.

Our calculated photoionization cross sections from four lowest bound excited ^1D states of Al^+ are shown in Fig. 1. The photoionization from $3p^2\ ^1D$ state leading to the higher

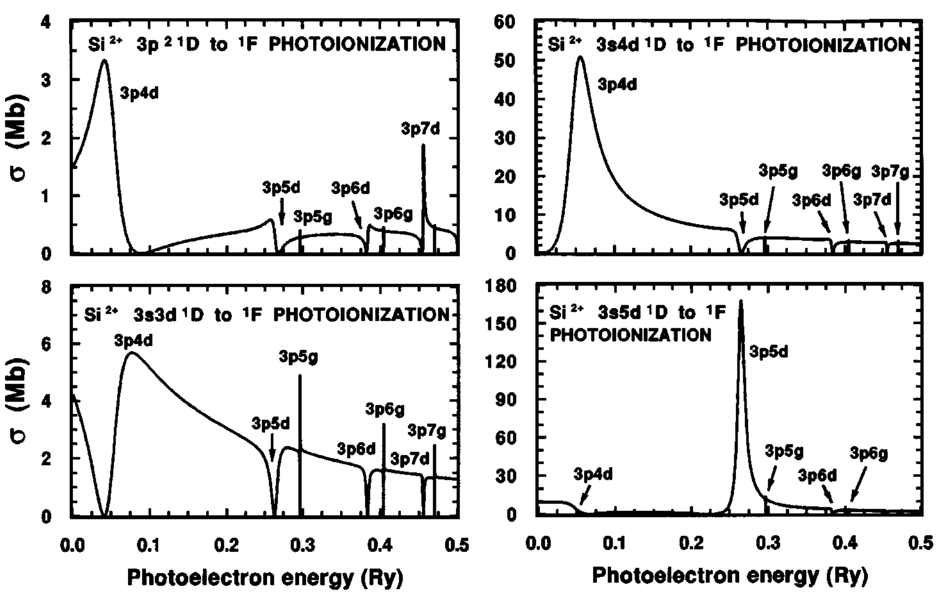

FIG. 2. Photoionization cross sections σ (in Mb) leading to the ^1F continuum from the bound excited ^1D states of Mg-like Si^{2+} ion.

TABLE II. The calculated widths Γ (in $a[\mu]=a\times 10^{\mu}$ Ry) and effective quantum numbers ν for the $3pnd$ and $3png$ ^1F resonances converging to the $3p$ limit. The energy differences between $3p$ and $3s$ limits, i.e., $\epsilon_{3p}-\epsilon_{3s}$, are 0.490 624 Ry and 0.652 434 Ry for Al^+ and Si^{2+}, respectively.

	Al^+		Si^{2+}	
State	ν	Γ	ν	Γ
$3p3d$	3.0883	5.6829[−2]		
$3p4d$	3.9952	3.2936[−2]	3.8681	3.2717[−2]
$3p5d$	4.9226	1.6098[−2]	4.8146	9.9168[−3]
$3p6d$	5.8834	7.5604[−3]	5.7858	3.4150[−3]
$3p7d$	6.8546	4.3188[−3]	6.7610	1.2386[−3]
$3p5g$	5.0194	3.7750[−5]	5.0283	5.8501[−5]
$3p6g$	6.0125	3.4866[−5]	6.0273	5.2279[−5]
$3p7g$	7.0035	2.6504[−5]	7.0269	4.2412[−5]

$3p\nu d$ ^1F states is primarily determined by the one-electron $3p\rightarrow\nu d$ transition. The strong initial-state mixing between the $3p^2$ and $3s3d$ configurations is reflected by the near-zero $3p^2$ $^1D\rightarrow 3p3d$ ^1F resonance due to the near cancellation between the *destructive* interference of (i) the direct $3p\rightarrow 3d$ transition from $3p^2$ to $3p3d$ configurations and (ii) the shakeup of the $3d$ electron following the $3s\rightarrow 3p$ core electron excitation from $3s3d$ to $3p3d$ configurations. In contrast, the photoionization from the $3s3d$ ^1D state is dominated by the strong $3p3d$ resonance resulting from the *constructive* interference between these two transitions. For photoionization from higher $3s\nu_i d$ ^1D states, the spectra are largely dominated by the shakeup of the outer d electron following the $3s\rightarrow 3p$ core electron excitation. The presence of a noticeable $3p3d$ ^1F resonance in higher $3s\nu d$ ^1D spectra further manifests the initial-state mixing between the $3sd$ and $3pp$ configuration series. The mixing between the $3sd$ and $3pp$ configurations is also responsible for the variation in oscillator strengths observed recently in the inner-shell excitation of Mg-like Al^+ and Si^{2+} [9].

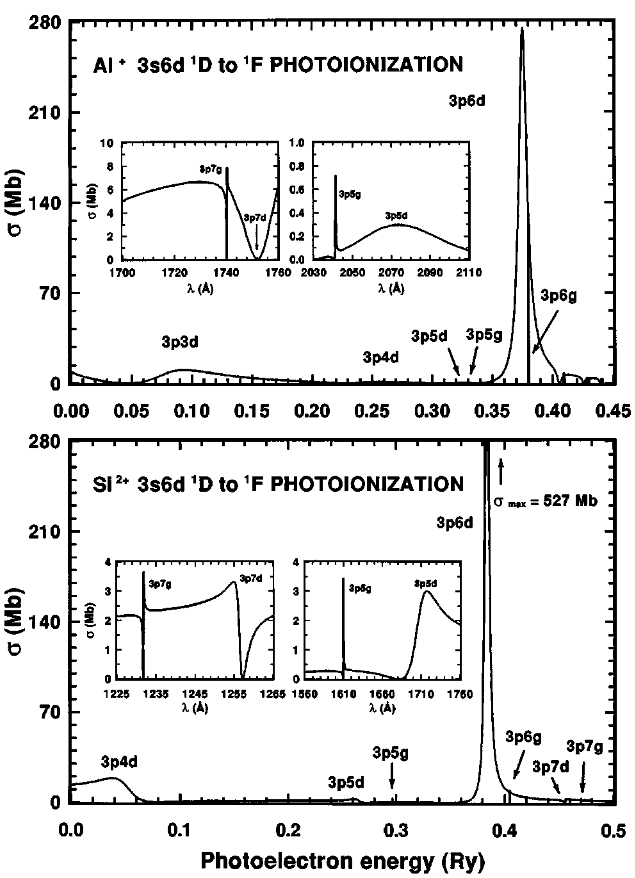

FIG. 3. Photoionization cross sections σ (in Mb) leading to the ^1F continuum from the bound excited $3s6d$ ^1D state of Mg-like Al^+ and Si^{2+} ions.

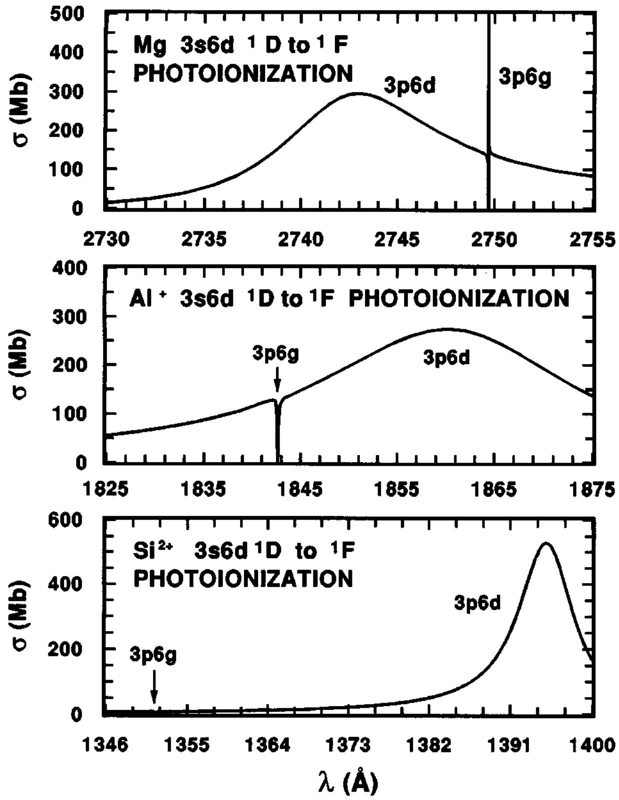

FIG. 4. The $3s6d$ $^1D\rightarrow 3p6l$ ^1F photoionization of Mg, Al^+, and Si^{2+}.

For Si^{2+} ion, the $3p3d$ ^1D state is *plunged* below the first ionization threshold. The calculated photoionization cross sections from four lowest bound excited ^1D states are shown in Fig. 2. Comparing with the Al^+ spectra, the energy separations between the $3p\nu d$ ^1F and $3p\nu g$ ^1F resonances are greater. For the broad $3p\nu d$ ^1F resonances, the small q (i.e., near *window* resonance) characteristic with zero cross section at or near the center of the resonance is more prominent than what appears in the Al^+ spectra.

Qualitatively, the peak cross section $\sigma_{\max}$ of a resonance should be inversely proportional to its resonant width [1,10]. Unlike the $^1D\rightarrow{}^1F$ resonant spectra in Mg [11], $\sigma_{\max}$ of the narrow $3p\nu g$ ^1F autoionization series of the Mg-like Al^+ and Si^{2+} ions are generally small in spite of their small widths, which are two to three orders of magnitude smaller than the $3p\nu d$ ^1F series (see, e.g., Table II). In addition, from the $3a5d$ ^1D spectra of both Al^+ and Si^{2+} shown in Figs. 1 and 2, the cross sections on the higher-energy side of the dominating $3p5d$ ^1Fpeak is greater than the ones on the

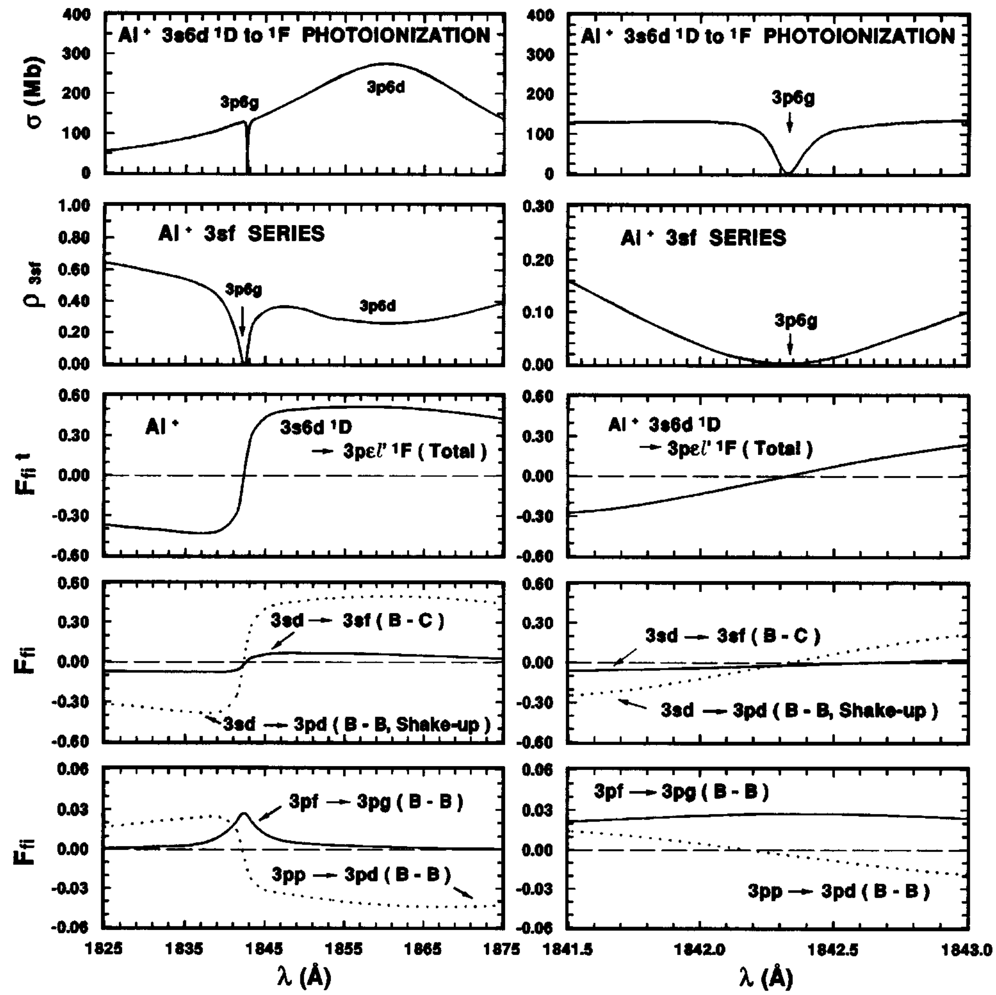

FIG. 5. The Al^+ $3s6d$ $^1D \rightarrow {}^1F$ photoionization near the $3p6d$ and $3p6g$ ^1F resonances and the individual contributions F_{fi} to the total transition amplitude F^t_{fi} from processes listed in Table I. Also given is the probability density ρ_{3sf}, defined by Eq. (79) of Ref. [6] or Eq. (10) of Ref. [5], for the $3sf$ ionization channel.

lower-energy side. This is also illustrated in the $3s6d$ ^1D spectra shown in Fig. 3. The calculated cross sections near the narrow $3p7g$ ^1F resonance on the higher-energy side of the dominating $3p6d$ ^1F peak is substantially greater than the ones near the narrow $3p5g$ ^1F resonance on the lower-energy side. Also, the broad $3p7d$ ^1F resonance on the higher-energy side is clearly characterized by a near-zero q parameter.

Detailed resonance profiles of the dominating $3s6d$ $^1D \rightarrow 3p6d$ ^1F shakeup structures of Mg, Al^+, and Si^{2+} are compared in Fig. 4. For Mg, the outer $6d$ orbital, which is subject to a slightly more screening by the inner $3s$ electron due to a substantial mixing between the $3p6d$ and the background $3s\epsilon f$ channel, does not penetrate as much to the smaller r region as the outer $6g$ orbital. As a result, the Mg $3p6d$ ^1F resonance is located at the higher-energy side of the $3p6g$ ^1F resonance. As the nuclear charge Z increases along the isoelectronic sequence, the nuclear Coulomb attraction eventually dominates over the small difference in mutual screening between outer and inner electrons due to

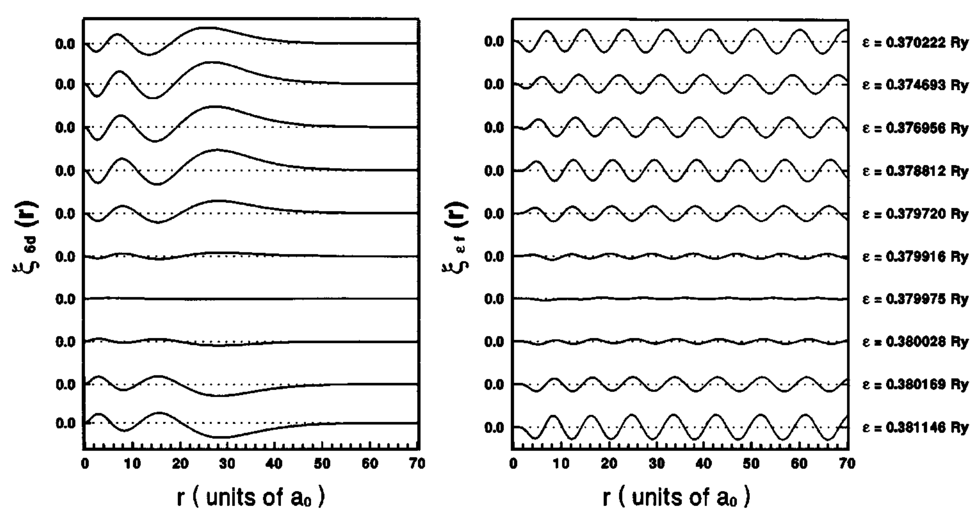

FIG. 6. The energy variations near the Al^+ $3p6d$ and $3p6g$ ^1F resonances for (i) the weighted final-state radial function ξ_{6d} and (ii) the oscillating function $\xi_{\epsilon f}$ for the outgoing photoelectron, defined by an expression similar to Eq. (50) of Ref. [6] or Eq. (10) of Ref. [5].

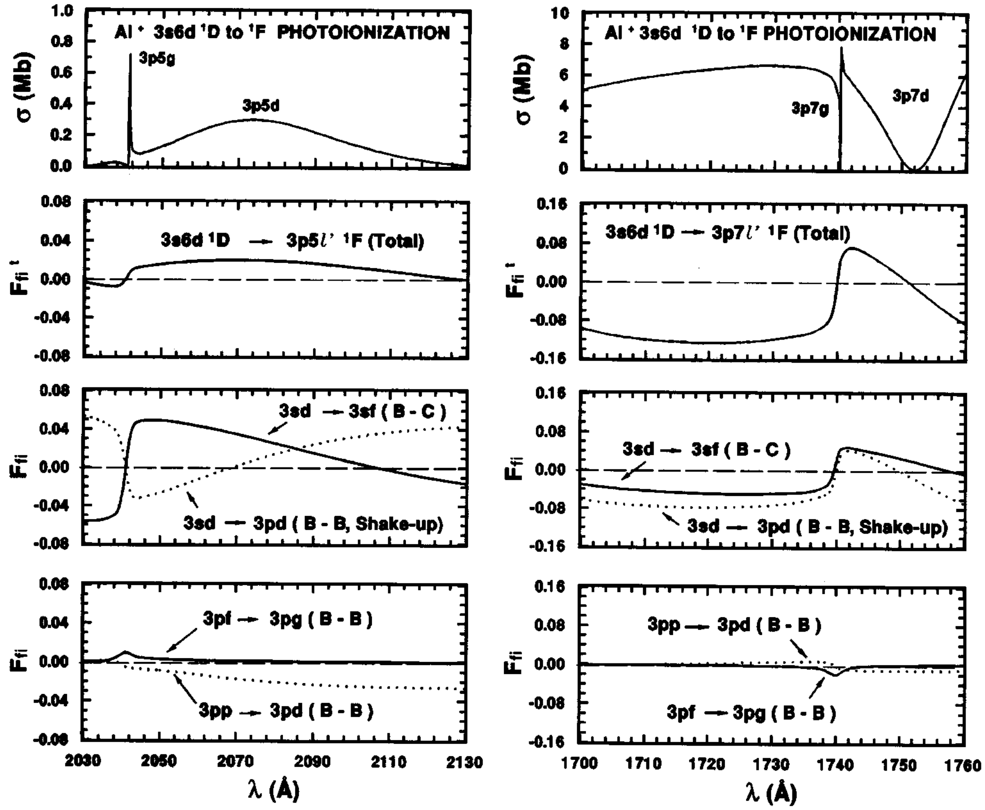

FIG. 7. The Al^+ $3s6d$ $^1D \rightarrow {}^1F$ photoionization near the $3p5l$ and $3p7l$ ^1F resonances and the individual contributions F_{fi} to the total transition amplitude F^t_{fi} from processes listed in Table I.

the configuration mixing and, as expected, the $3p6d$ ^1F resonances for Al^+ and Si^{2+} *plunge* below the $3p6g$ ^1F resonances.

III. DISCUSSIONS

A detailed breakdown of individual contributions to F^t_{fi}, shown in Fig. 5, from the four processes listed in Table I indicates a strong dominance of the bound-to-bound shakeup process in the Al^+ $3s6d$ $^1D \rightarrow 3p6l$ ^1F photoionization. The $3p6d$ and $3p6g$ ^1F resonances can also be identified by the local minima in the probability density ρ_{3sf} for the $3sf$ ionization channel. Whereas the $3p6g$ configuration accounts for nearly 100% of the probability density of the narrow $3p6g$ ^1F resonance, the mixing between the $3pd$ and $3sf$ configuration series is substantial (i.e., 30% or more for the $3sf$ series) for the $3p6d$ ^1F resonance. The cross section near the $3p6g$ ^1F *window* resonance, shown in detail from the figure on the right, reaches a zero at the resonance due to the sign change of F^t_{fi}, or, equivalently, the sign change in F_{fi} corresponding to the bound-to-bound shakeup process. Since the weighted radial function ξ_{6d} corresponding to the $3p6d$ ^1F resonance is the only energy-dependent part of the shakeup amplitude, i.e., $\xi_{\nu d}$ in $\langle \chi_{3s}|r|\chi_{3p}\rangle\langle \xi_{\nu_i d}|\xi_{\nu d}\rangle$, the sign change in F_{fi} can only result from the energy variation of ξ_{6d} in the vicinity of the $3p6g$ ^1F resonance. The radial functions ξ_{6d}, representing the final-state $6d$ electron, together with the oscillating functions $\xi_{\epsilon f}$ which represent the outgoing photoelectron, are plotted in Fig. 6 at energies across the $3p6d$ and $3p6g$ ^1F resonances. At the $3p6g$ ^1F resonance, i.e., at E_r=0.379 975 Ry, the energy-dependent amplitudes of both ξ_{6d} and $\xi_{\epsilon f}$ reach a minimum. Similar to the sign change of the oscillating function $\xi_{\epsilon l}$ due to the rapid increase of the scattering phase shift by a total of π across the resonance (see, e.g., Fig. 2 of Ref. [4]), the sign of ξ_{6d} corresponding to the $3p6d$ ^1F resonance is also reversed as energy increases across the narrow $3p6g$ ^1F resonance. In addition, as expected, the oscillating functions $\xi_{\epsilon f}$ on the opposite sides of the $3p6d$ and $3p6g$ ^1F resonances at ϵ=0.370 222 Ry and ϵ=0.381 146 Ry are nearly identical, except an increase of the scattering phase shift by a total of 2π across both $3p6d$ ^1F(at E_r=0.375 065 Ry) and $3p6g$ ^1F (at E_r=0.379 975 Ry) resonances.

For Mg, a similar breakdown of the contributions to F^t_{fi} from individual process near the $3p6g$ ^1F resonance shows that the dominance of the shakeup process remains. However, a slight shift in the zero in F^t_{fi} from the minimum in ρ_{3sf} has led to a strongly asymmetric resonant structure. For Si^{2+}, the $3p6g$ ^1F is sufficiently separated from the $3p6d$ ^1F resonance. As a result, F^t_{fi} is no longer dominated by a single process.

Figure 7 presents a detailed breakdown of individual contributions to the total transition amplitude F^t_{fi} from the four processes listed in Table I for the Al^+ $3s6d$ $^1D \rightarrow {}^1F$ photoionization near the $3p5l$ and $3p7l$ ^1F resonances. Unlike the strong $\Delta\nu$=0 transition (e.g., $3s6d$ $^1D \rightarrow 3p6d$ ^1F photoionization), the transition amplitude is no longer dominated by the bound-to-bound shakeup process involving the $6d$ electron due to a substantially smaller overlapping integral $O_{\nu\nu_i}=\langle \xi_{\nu_i d}|\xi_{\nu d}\rangle$ between the weighted radial functions of the initial and final d electrons. In fact, for the $3s6d$ $^1D \rightarrow 3p5l$ ^1F photoionization, the cross sections near the $3p5g$ ^1F resonance is substantially reduced due to a *destructive* interference between the bound-to-bound $3s6d \rightarrow 3p5d$ shakeup process and the bound to continuum

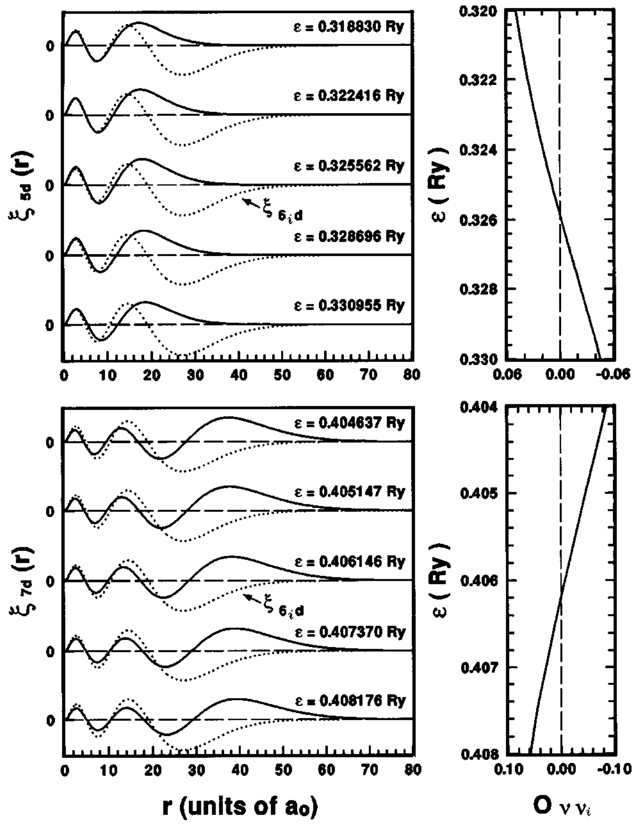

FIG. 8. Comparison of the weighted final-state radial functions ξ_{5d} and ξ_{7d} near the Al^{+} $3p5d$ and $3p7d$ ^1F resonances, respectively, with the weighted initial-state radial function ξ_{6_id}. The overlapping integrals between $\xi_{\nu d}$ and $\xi_{\nu_i d}$ are given by $O_{\nu\nu_i} = \langle \xi_{\nu_i d} | \xi_{\nu d} \rangle$. The weighted radial functions are defined by an expression similar to Eq. (50) of Ref. [6] or Eq. (10) of Ref. [5].

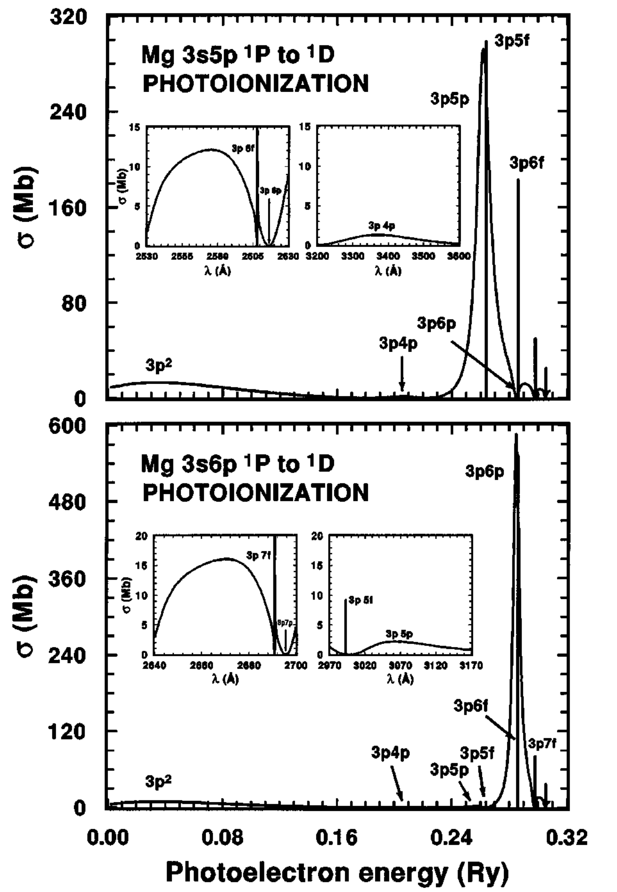

FIG. 9. Photoionization cross sections σ (in Mb) leading to the ^1D continuum from the bound excited $3s\nu_i p$ ^1P states of Mg atom.

$3s6d \rightarrow 3s\epsilon f$ direct transition. On the other hand, the cross sections near the $3s6d$ $^1D \rightarrow 3p7g$ ^1F photoionization is clearly enhanced due to a *constructive* interference between the bound-to-bound $3s6d \rightarrow 3p7d$ shakeup process and the bound-to-continuum $3s6d \rightarrow 3s\epsilon f$ direct transition.

The energy variation of the transition amplitude F_{fi} of the bound-to-bound $3s\nu_i d \rightarrow 3p\nu d$ shakeup process is determined by the overlapping integral $O_{\nu\nu_i}$ between the weighted radial functions of the initial and final d electrons. Following our earlier discussion, the integral $O_{\nu\nu_i}$ changes its sign at the $3p\nu g$ ^1F resonance due to the sign change of the weighted final-state radial function $\xi_{\nu d}$ (see, e.g., Fig. 6). Our calculation has also shown that the final-state radial functions $\xi_{\nu d}$ expands slowly outwards as energy increases (see, e.g., Fig. 8). Except for the $\Delta\nu=0$ transition, the overlapping integral $O_{\nu\nu_i}$ is generally small due to the quasiorthogonality between the initial- and final-state weighted radial d functions. In fact, it changes sign at an energy close to the center of the $3p\nu d$ ^1F resonance. In other words, whereas for a $\Delta\nu=0$ transition, the transition amplitude F_{fi} for the bound-to-bound shakeup process changes sign only *once* near the $3p\nu g$ ^1F resonance, F_{fi} is expected to change sign *twice* for all $\Delta\nu\neq 0$ transitions, i.e., first near the $3p\nu d$ ^1F resonance, then at the $3p\nu g$ ^1F resonance. In contrast, for the direct bound-to-continuum $3s\nu_i d \rightarrow 3s\epsilon f$ transition, the transition amplitude $F_{fi} = \langle \xi_{\nu_i d} | r | \xi_{\epsilon f} \rangle$ always changes its sign *twice* as the photon energy increases across the $3p\nu d$ and $3p\nu g$ ^1F resonances due to the sign change of the oscillating function $\xi_{\epsilon f}$ as the scattering phase shift increases by π for each resonance (see, e.g., Fig. 6).

As a result, the relative sign between the transition amplitudes, corresponding to the bound-to-bound $3s\nu_i d \rightarrow 3p\nu d$ shakeup process and the bound-to-continuum $3s\nu_i d \rightarrow 3s\epsilon f$ direct transition, reverses as the energy increases across the dominating shakeup structure (see, e.g., Fig. 7). And, the autoionization profiles shown in Fig. 3 changes completely due to the reversal of the interference between the bound-to-bound and the bound-to-continuum contributions shown in Fig. 7. In addition, at energies near the broad resonance (e.g., the $3p7d$ ^1F resonance shown in Fig. 7) above the dominating shakeup structure, the additional constructive contribution due to the bound-to-bound $3s\nu_i d \rightarrow 3p\nu d$ shakeup process does not change the overall qualitative features of the total transition amplitude F^t_{fi} from the bound-to-continuum $3s\nu_i d \rightarrow 3s\epsilon f$ direct transition. Consequently, similar to a photoionization dominated by a direct bound-to-continuum transition, the broad $3p\nu d$ ^1F resonance on the higher side is characterized by a near-zero q parameter shown in Figs. 3 and 7. The substantial change in the resonance features between the autoionization states at energies below and above the dominating shakeup structure is not limited to the $^1D \rightarrow {}^1F$ photoionization. In fact, similar feature is also found in photoionization leading to a lower angular momentum state, such as the Mg $3s\nu_i p$ $^1P \rightarrow {}^1D$ spectra shown in Fig. 9.

ACKNOWLEDGMENTS

This work was supported by NSF under Grant No. PHY94-13338 and by KAERI and the Center for Molecular Science at KAIST of Korea.

[1] U. Fano, Phys. Rev. **124**, 1866 (1961).

[2] J. M. Esteva, G. Mehlman-Balloffet, and J. Romand, J. Quant. Spectrosc. Radiat. Transfer **12**, 1291 (1972); G. Mehlman-Balloffet and J. M. Esteva, Astrophys. J. **157**, 945 (1969).

[3] T. N. Chang and L. Zhu, Phys. Rev. A **48**, R1725 (1991).

[4] T. N. Chang and L. Zhu, Phys. Rev. A **51**, 374 (1995).

[5] T. N. Chang and X. Tang, Phys. Rev. A **44**, 232 (1991).

[6] T. N. Chang, in *Many-body Theory of Atomic Structure and Photoionization*, edited by T. N. Chang (World Scientific, Singapore, 1993), p. 213.

[7] T. A. Carlson and M. O. Krause, Phys. Rev. **140**, A1057 (1965); T. A. Carlson, *ibid*. **156**, 142 (1967); W. E. Cooke, T. F. Gallagher, S. A. Edelstein, and R. M. Hill, Phys. Rev. Lett. **41**, 178 (1978); R. M. Jopson, R. R. Freeman, W. E. Cooke, and J. Bokor, *ibid*. **51**, 1640 (1983); K. Butler, C. Mendoza, and C. J. Zeippen, J. Phys. B **26**, 4409 (1993).

[8] T. N. Chang and T. K. Fang, Phys. Rev. A **52**, 2638 (1995).

[9] M. H. Sayyar, E. T. Kennedy, L. Kiernan, J.-P. Mosnier, and J. T. Costello, J. Phys. B **28**, 1715 (1995).

[10] T. N. Chang, Phys. Rev. A **37**, 4090 (1988).

[11] T. N. Chang and X. Tang, Phys. Rev. A **38**, 1258 (1988).